

Electronic Supplementary Information for

Efficient iron-cobalt oxide bifunctional electrode catalyst in rechargeable high current density zinc-air battery

Wei Jian Sim,^a Mai Thanh Nguyen,^{a,*} Zixuan Huang,^a Soorathee Kheawhom,^b Chularat Wattanakit,^c Tetsu Yonezawa^{a,*}

^aDivision of Materials Science and Engineering, Faculty of Engineering, Hokkaido University, Kita 13 Nishi 8, Kita-ku, Sapporo, Hokkaido 060-8628, Japan

^bDepartment of Chemical Engineering, Faculty of Engineering, Chulalongkorn University, Payathai Road Pathumwan, Bangkok 10330, Thailand

^cVidyasirimedhi Institute of Science and Technology, Wangchan Valley 555 Moo 1 Payupnai, Wangchan, Rayong 21210, Thailand

*Corresponding Author, email: tetsu@eng.hokudai.ac.jp, mai_nt@eng.hokudai.ac.jp

Table of content

Fig. S1 TEM micrograph of FeCo oxide sintered with graphite.

Fig. S2 Representative charge/discharge profiles of ZABs using FeCo 0 wt% catalyst.

Fig. S3 Representative charge/discharge profiles of ZABs using FeCo 10 wt% catalyst.

Fig. S4 Representative charge/discharge profiles of ZABs using FeCo 20 wt% catalyst.

Fig. S5 Representative charge/discharge profiles of ZABs using FeCo 50 wt% catalyst.

Fig. S6 Representative charge/discharge profiles of ZABs using FeCo 60 wt% catalyst.

Fig. S7 Representative charge/discharge profiles of ZABs using FeCo 100 wt% catalyst.

Fig. S8 Number of discharging/charging cycles for various FeCo loading level evaluated at 95 % and 85 % discharge capacity.

Fig. S9 UV-vis of electrolyte at 10 times dilution after 0, 3, 7, 11 and 23 cycles of discharging and charging in a ZAB with FeCo 40 wt%.

Fig. S10 Gas diffusion layer of a ZAB with FeCo 40 wt% observed with an optical microscope at magnification×20.

Fig. S11 CV of FeCo 10 wt%, FeCo 20 wt%, FeCo 50 wt%, and FeCo 60 wt%.

Fig. S12 LSV of FeCo 0 wt%, FeCo 10 wt%, FeCo 20 wt%, FeCo 50 wt%, FeCo 60 wt%, and FeCo 100 wt%.

Fig. S13 Discharge potentials at the start of each cycle for FeCo 0 wt%, FeCo 10 wt%, FeCo 20 wt%, FeCo 40 wt%, FeCo 50 wt%, FeCo 60 wt%, and FeCo 100 wt%.

The Koutecký–Levich equation and parameters

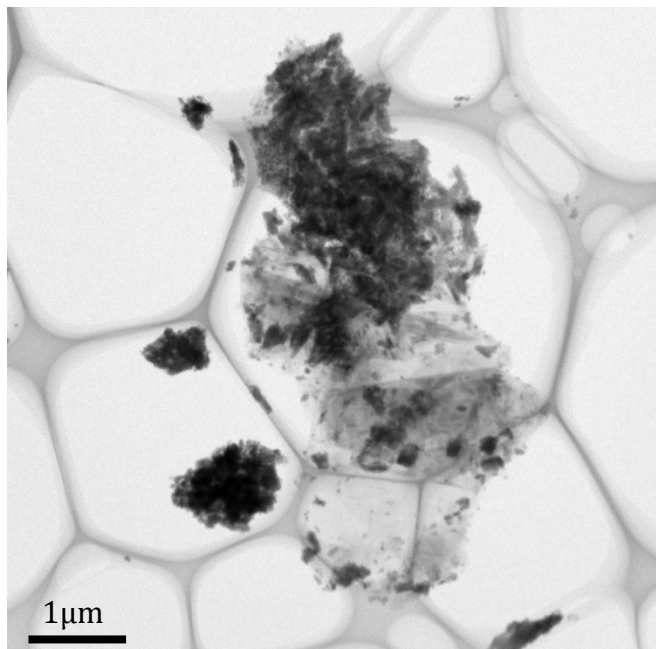


Fig. S1 TEM micrograph of FeCo oxide sintered with graphite. Concentrations of dark contrast indicate agglomeration of metal oxides where areas with low contrast suggest absence of metal oxides.

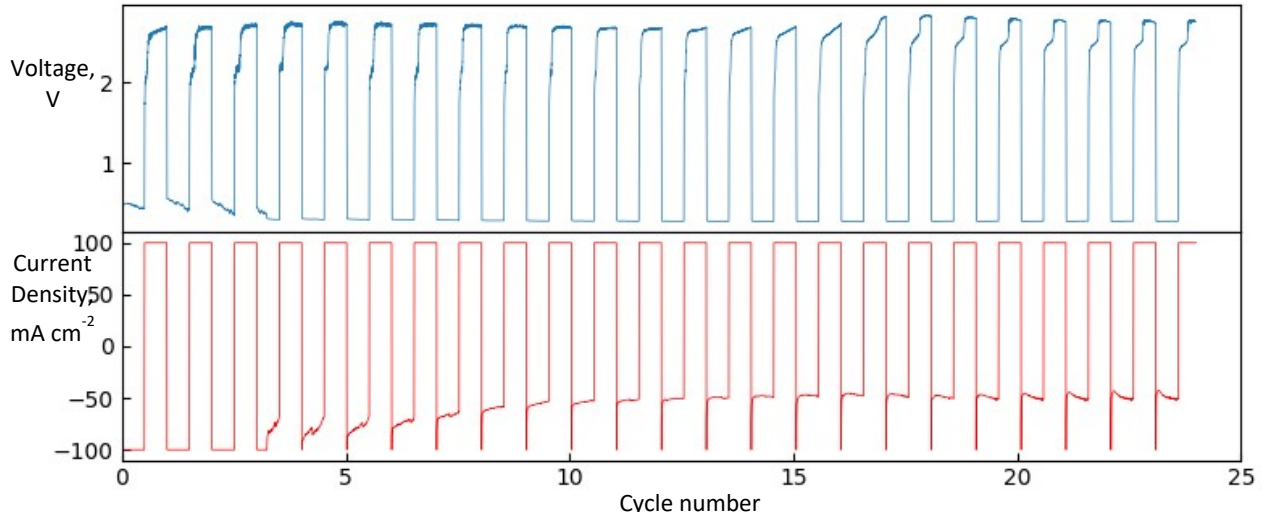


Fig. S2 Representative charge/discharge profiles of ZABs using FeCo 0 wt% catalyst.

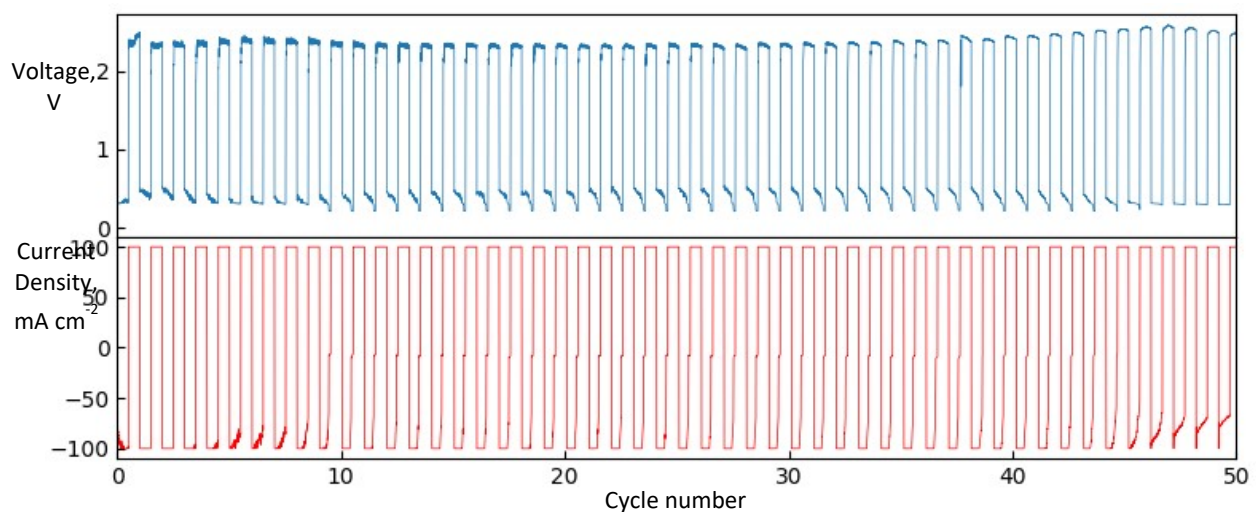


Fig. S3 Representative charge/discharge profiles of ZABs using FeCo 10 wt% catalyst.

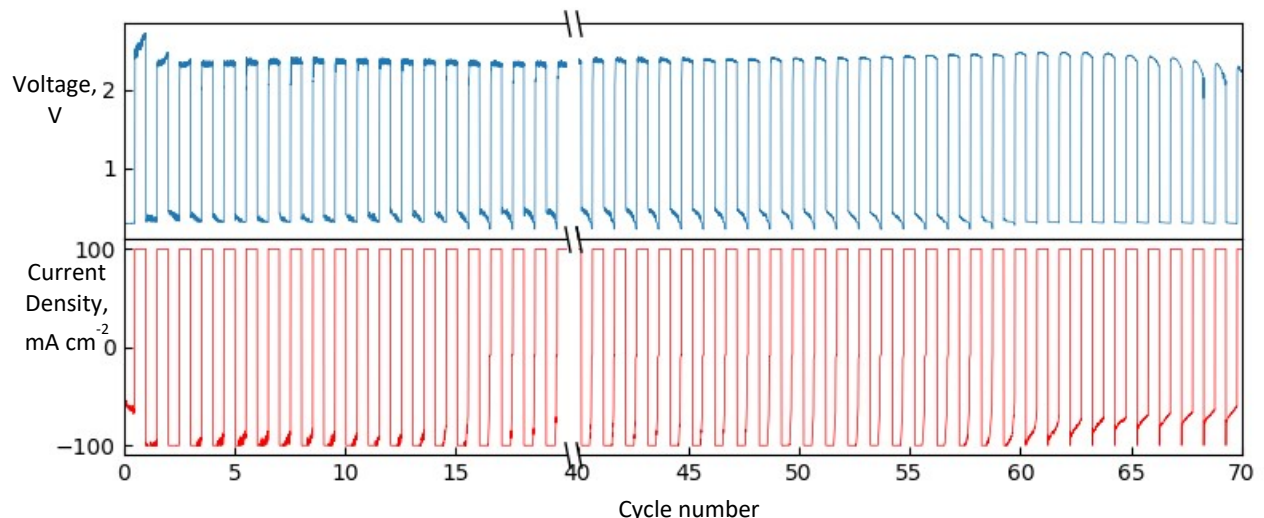


Fig. S4 Representative charge/discharge profiles of ZABs using FeCo 20 wt% catalyst.

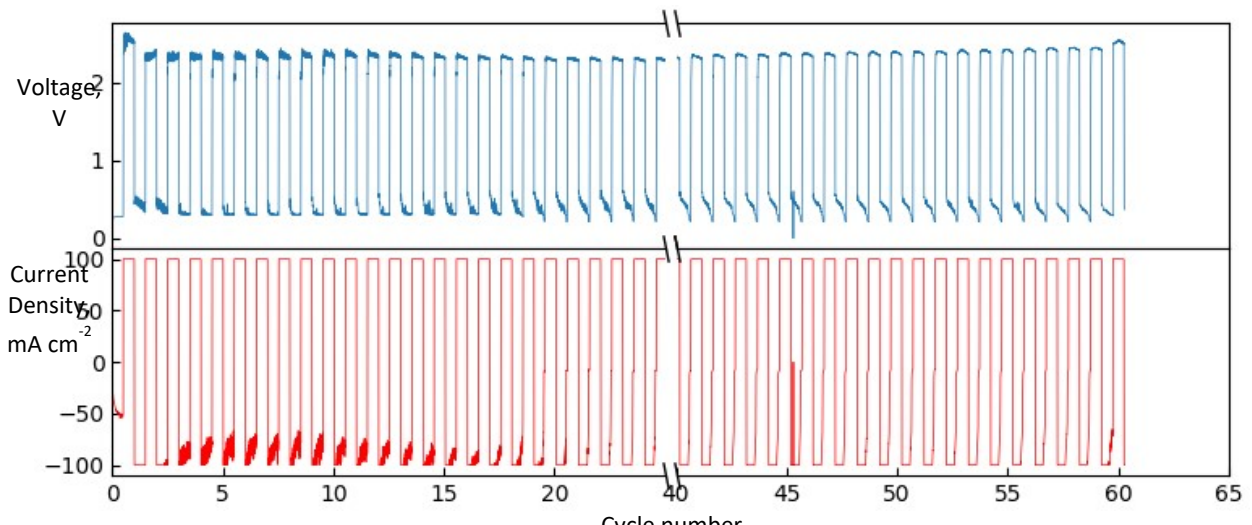


Fig. S5 Representative charge/discharge profiles of ZABs using FeCo 50 wt% catalyst.

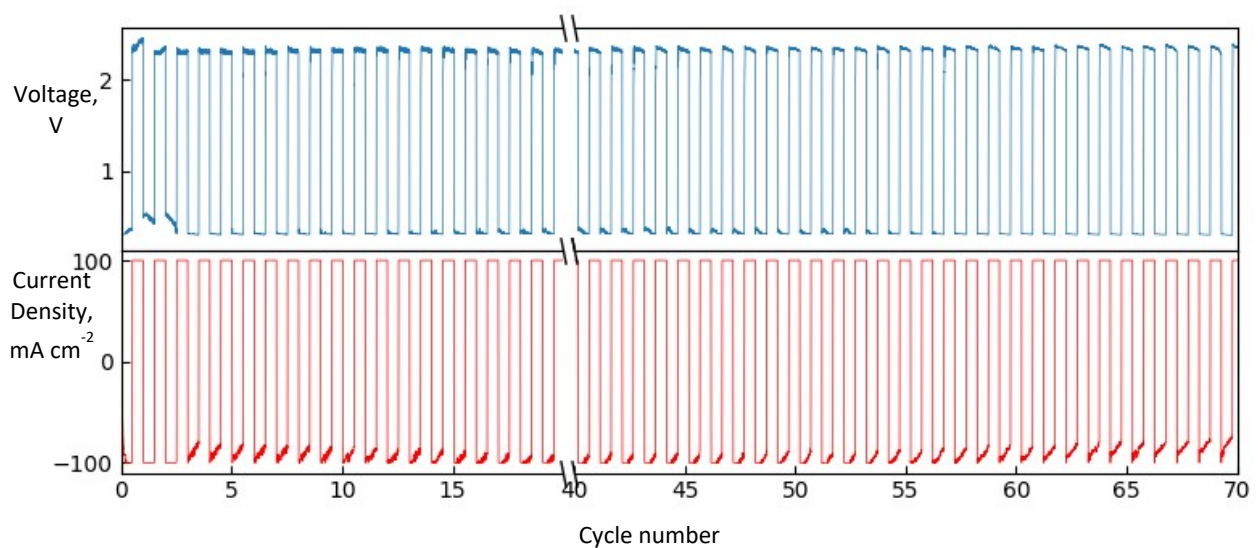


Fig. S6 Representative charge/discharge profiles of ZABs using FeCo 60 wt% catalyst.

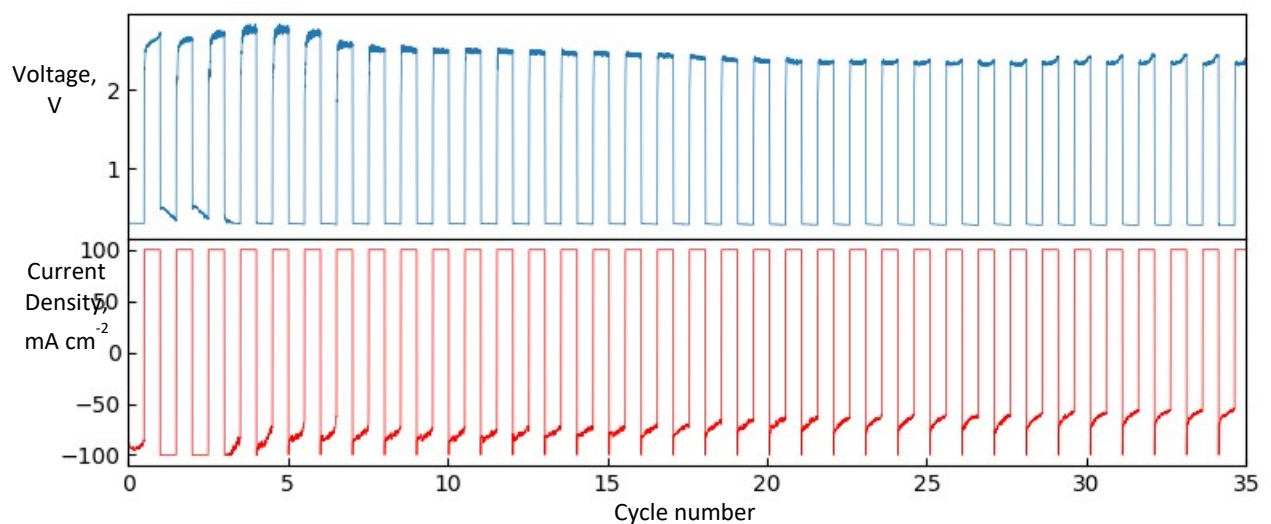
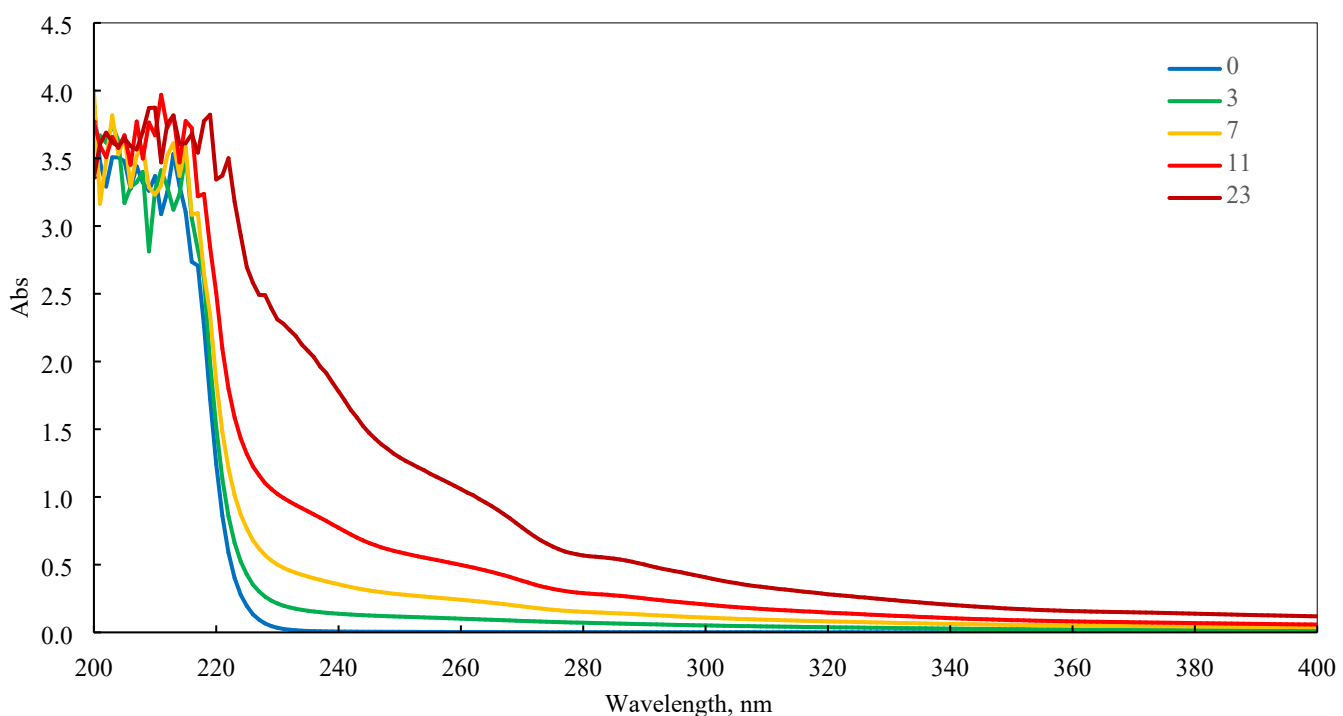
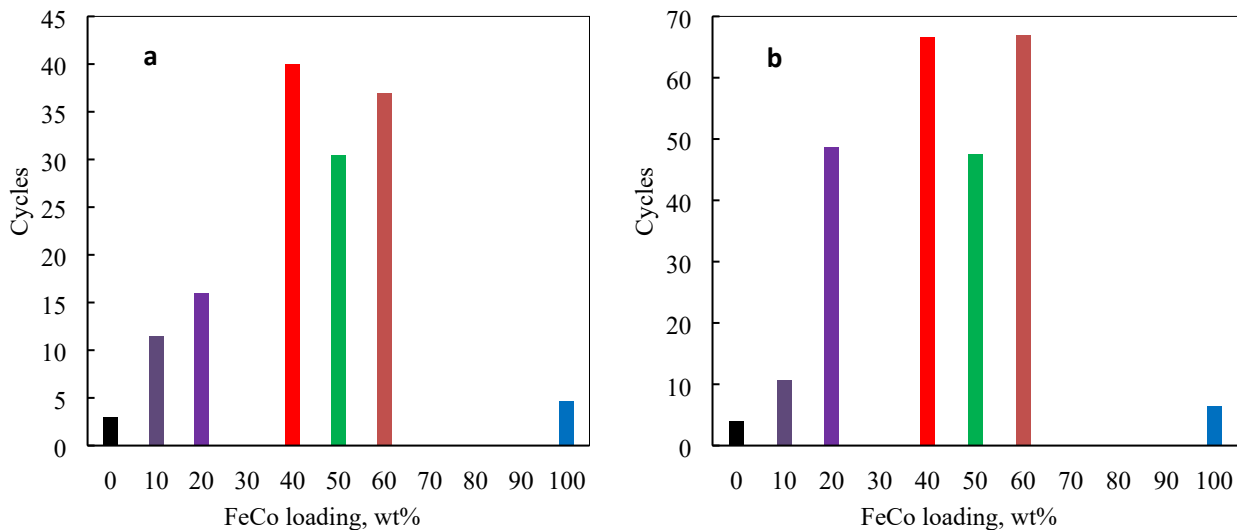


Fig. S7 Representative charge/discharge profiles of ZABs using FeCo 100 wt% catalyst.



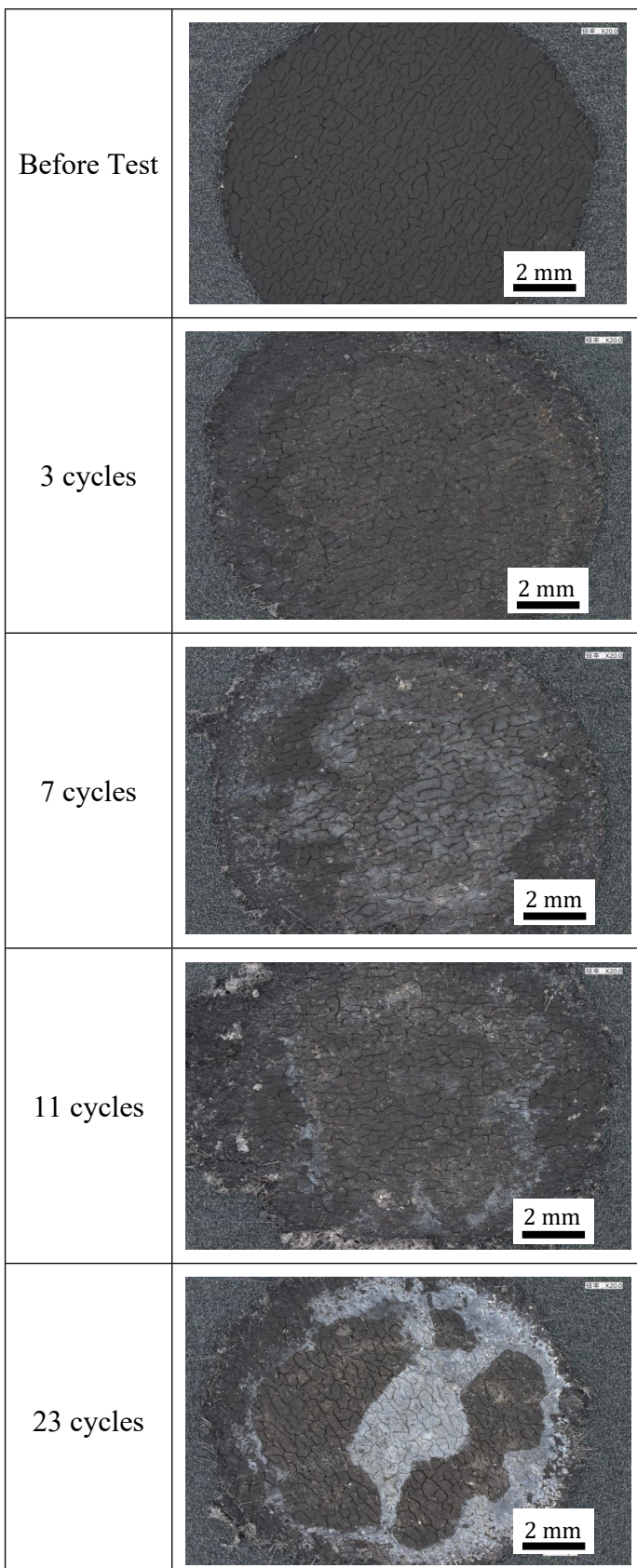


Fig. S10 Gas diffusion layer of a ZAB with FeCo 40 wt% observed with an optical microscope at magnification $\times 20$.

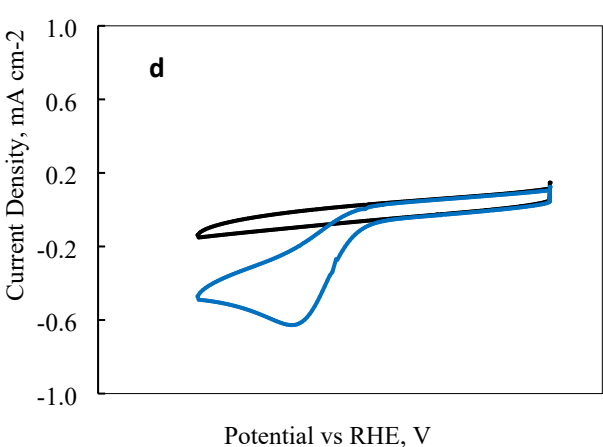
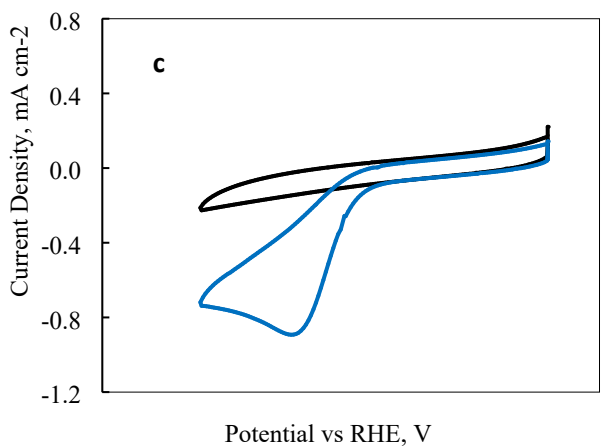
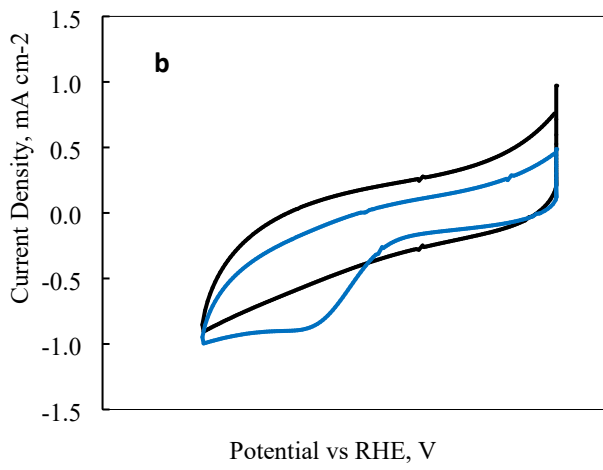
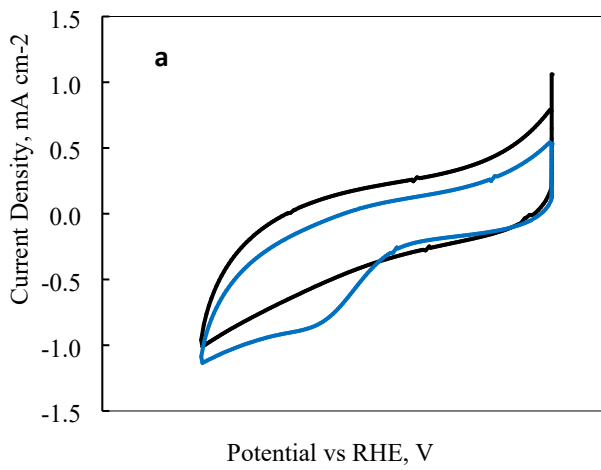


Fig. S11 CV of (a) FeCo 10 wt%, (b) FeCo 20 wt%, (c) FeCo 50 wt%, and (d) FeCo 60 wt% in saturated Ar electrolyte (black line) and saturated O₂ electrolyte (blue line). Scan rate was 50 mV s⁻¹, in 1.0 M KOH with a stationary RDE.

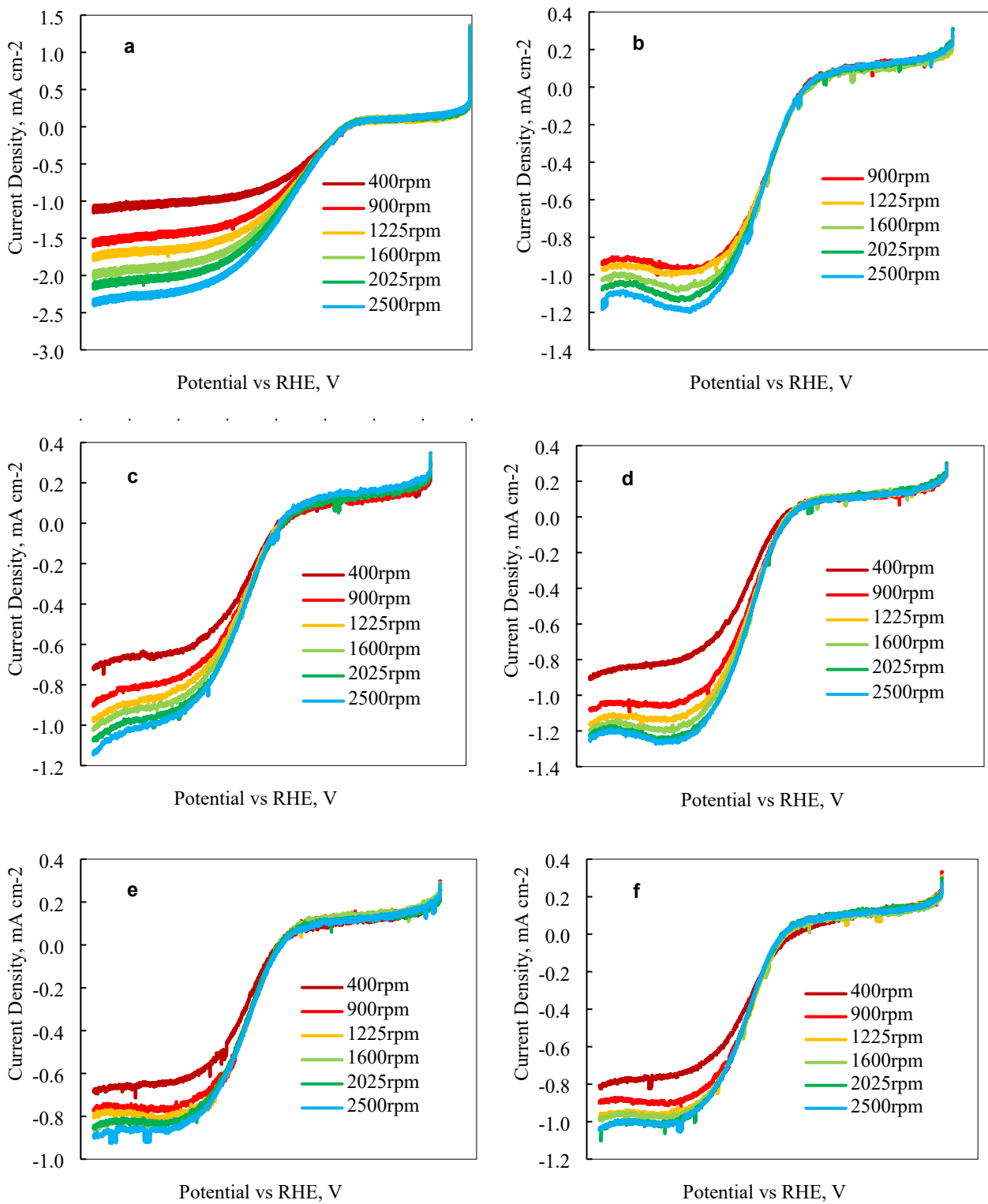


Fig. S12 LSV of (a) FeCo 0 wt%, (b) FeCo 10 wt%, (c) FeCo 20 wt%, (d) FeCo 50 wt%, (e) FeCo 60 wt%, and (f) FeCo 100 wt% with RDE rotation speed at 400 rpm (dark red), 900 rpm (red), 1225 rpm (yellow), 1600 rpm (light green), 2025 rpm (green) and 2500 rpm (blue).

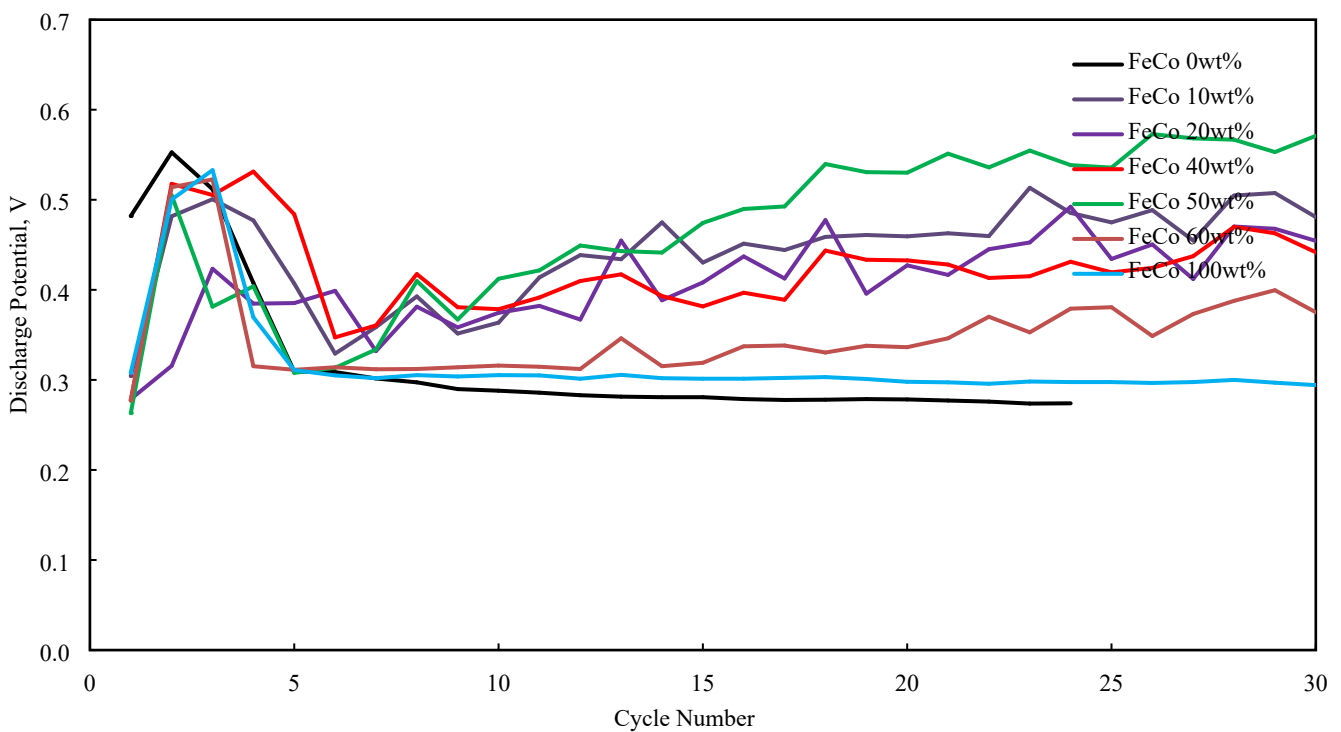


Fig. S13 Discharge potentials at the start of each cycle for FeCo 0 wt% (black), FeCo 10 wt% (brown), FeCo 20 wt% (purple), FeCo 40 wt% (red), FeCo 50 wt% (green), FeCo 60 wt% (orange), and FeCo 100 wt% (blue). Potential was allowed to stabilise for 5 min before measurements were taken.

The Koutecký–Levich equation and parameters

In a rotating disc electrode (RDE) setup, the Koutecký–Levich equation can be expressed as, (1)

$$\frac{1}{j} = \frac{1}{j_k} + \frac{1}{B_L \omega^2}$$

where j is the measured current, j_k is the kinetic current from redox reactions, ω is the rotation speed of the RDE, and B_L is the Levich constant. This form is valid for the diffusion limited region of the linear scan voltammetry (LSV) where kinetic current is independent of applied potential and measured current is only a function of ω .

By plotting $1/j$ against $1/\omega^{1/2}$, the gradient of the linear plots, $1/B_L$ can be extracted and the electron transfer number can be calculated according to Levich equation.

$$B_L = 0.2nFD_0^{\frac{2}{3}}v^{-\frac{1}{6}}C_0$$

(B is expressed for ω in rpm)

The parameters used in the calculations were reported by Gubbins and Walker (2) and applied by Yuan et al (3).

F = Faraday constant = 96485 C mol⁻¹
 D = diffusion coefficient = 1.65×10^{-5} cm² s⁻¹
 v = kinematic viscosity = 0.95×10^{-2} cm² s⁻¹
 C = analyte concentration = 0.83×10^{-6} mol cm⁻³

References

1. B. G. Lević, Physicochemical Hydrodynamics; Prentice-Hall, 1962.
2. K. E. Gubbins and R. D. Walker, The Solubility and Diffusivity of Oxygen in Electrolytic Solutions. *J. Electrochem. Soc.* **1965**, *112*, 469, DOI: 10.1149/1.2423575
3. X. Yuan, X. Li, W. Qu, D. G. Ivey, and H. Wang, Electrocatalytic Activity of Non-Stoichiometric Perovskites toward Oxygen Reduction Reaction in Alkaline Electrolytes. *ECS Trans.* **2011**, *35* (33), 11-20, DOI: 10.1149/1.3655433